Science
AAAS

Supplementary Materials for

Distinct roles for precession, obliquity, and eccentricity in Pleistocene 100-kyr glacial cycles

Stephen Barker *et al*.

Corresponding author: Stephen Barker, barkers3@cf.ac.uk

Science **387**, eadp3491 (2025)
DOI: 10.1126/science.adp3491

The PDF file includes:

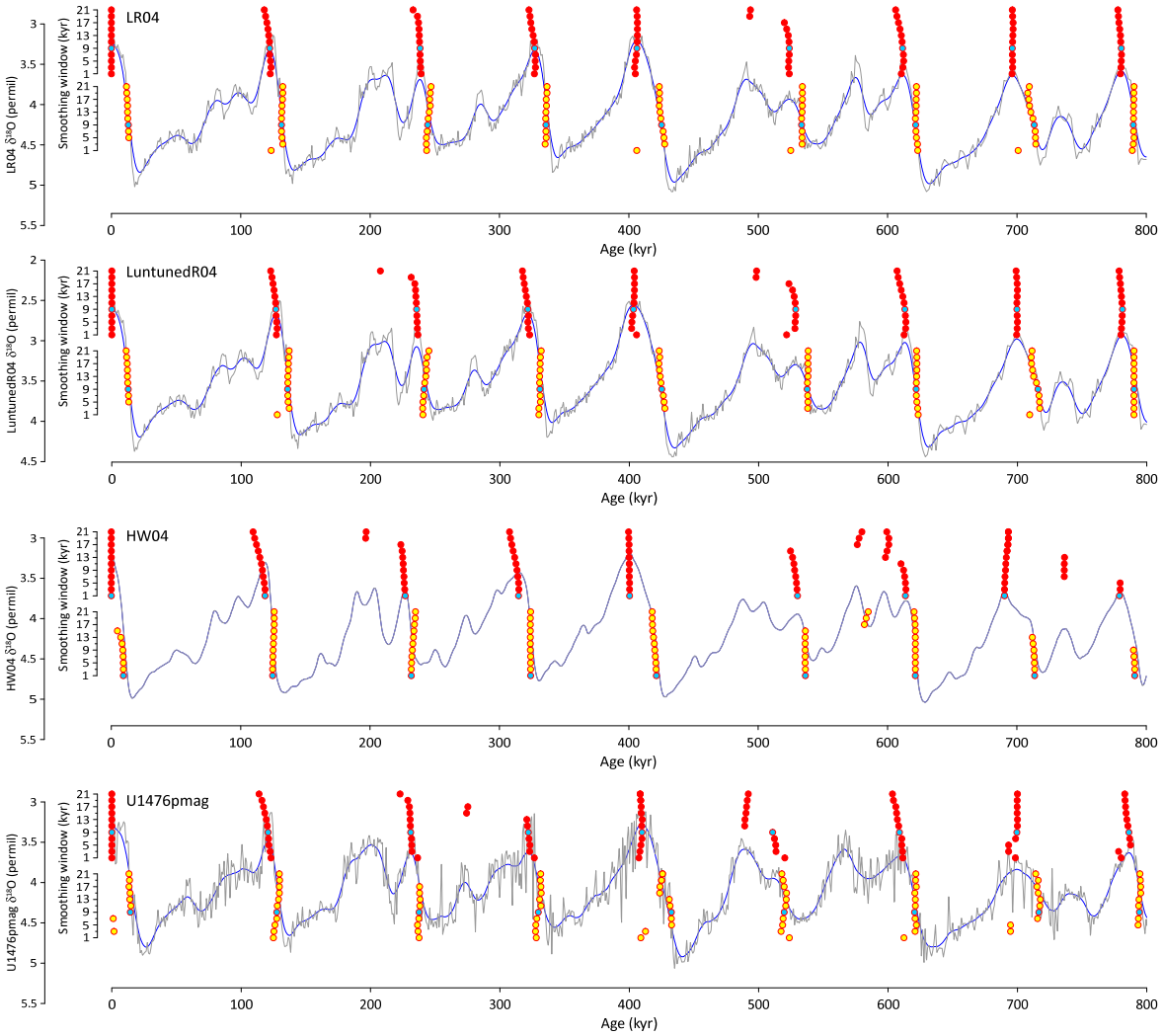

Fig. S1. Effect of smoothing window length on the timing of Peak IG and Max deglac. Red and yellow symbols represent Peak IG and Max deglac (respectively) for various smoothing windows (1:2:21kyr) of each curve. Blue symbols represent window length adopted in this study (9kyr for LR04, LR04_untuned and U1476pmag, 1kyr for HW04). Blue curve in each panel is the relevant record smoothed according to the specified window length. Grey curve is raw stack/record (HW04 is already smoothed).

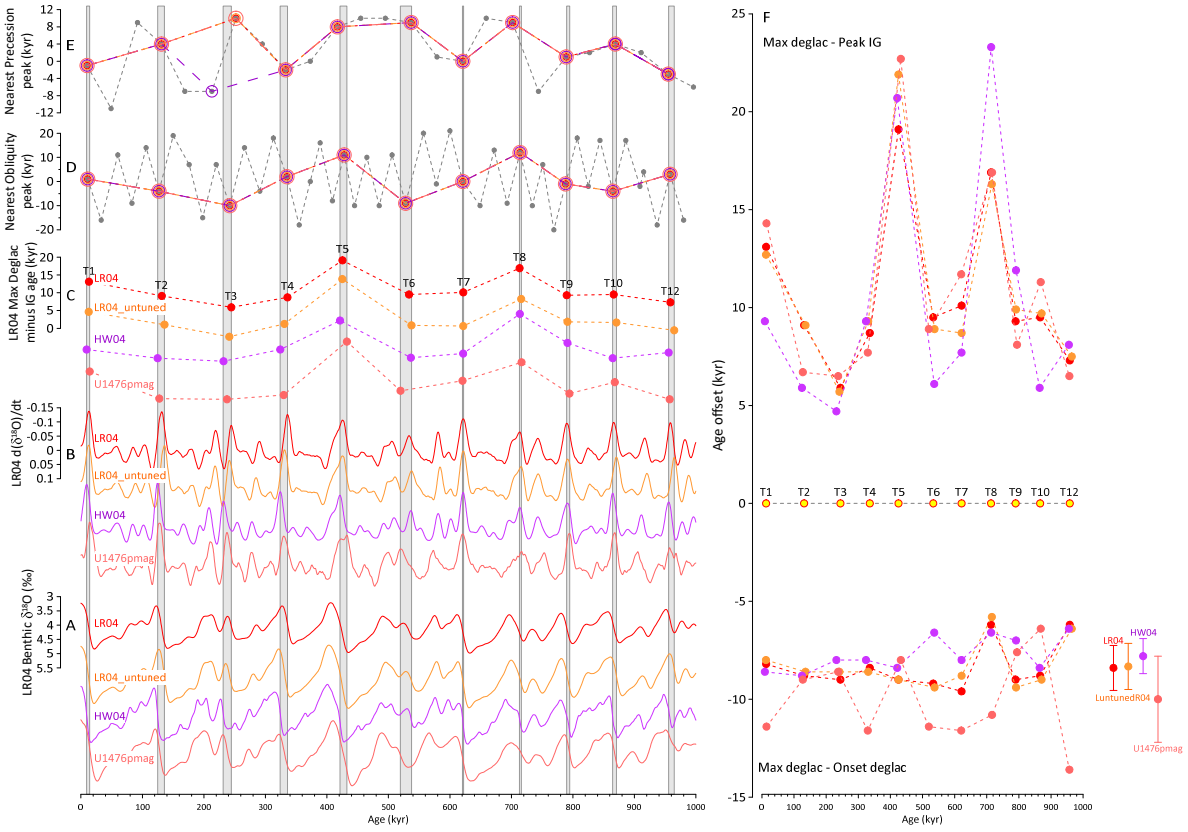

Fig. S2. Summary of results for 3 records/stacks of benthic $\delta^{18}O$ on 4 independent age models. (A) Smoothed records/stacks of benthic $\delta^{18}O$ (B) First differential of $\delta^{18}O$ (C) Max deglac minus Peak IG reveals similar variations among the 4 records/timescales (D) Grey symbols show the offset between each precession peak over past 1Myr and its nearest obliquity neighbour. Coloured symbols highlight those precession peaks that are closest to each Max deglac (the same precession peaks are selected for all records/timescales). Note the similar relationship between deglacial duration (C; Max deglac – Peak IG) and precession-obliquity (in D) as observed for the LR04 stack and shown in Fig. 1. See also Figs. 2, S3, S4. (E) Same as (D) but for obliquity. The same obliquity peaks are selected for each record except HW04 for T3, which is closer to a later obliquity peak than the other records. (F) The duration between Onset deglac and Max deglac is relatively invariant as compared with Max deglac – Peak IG.

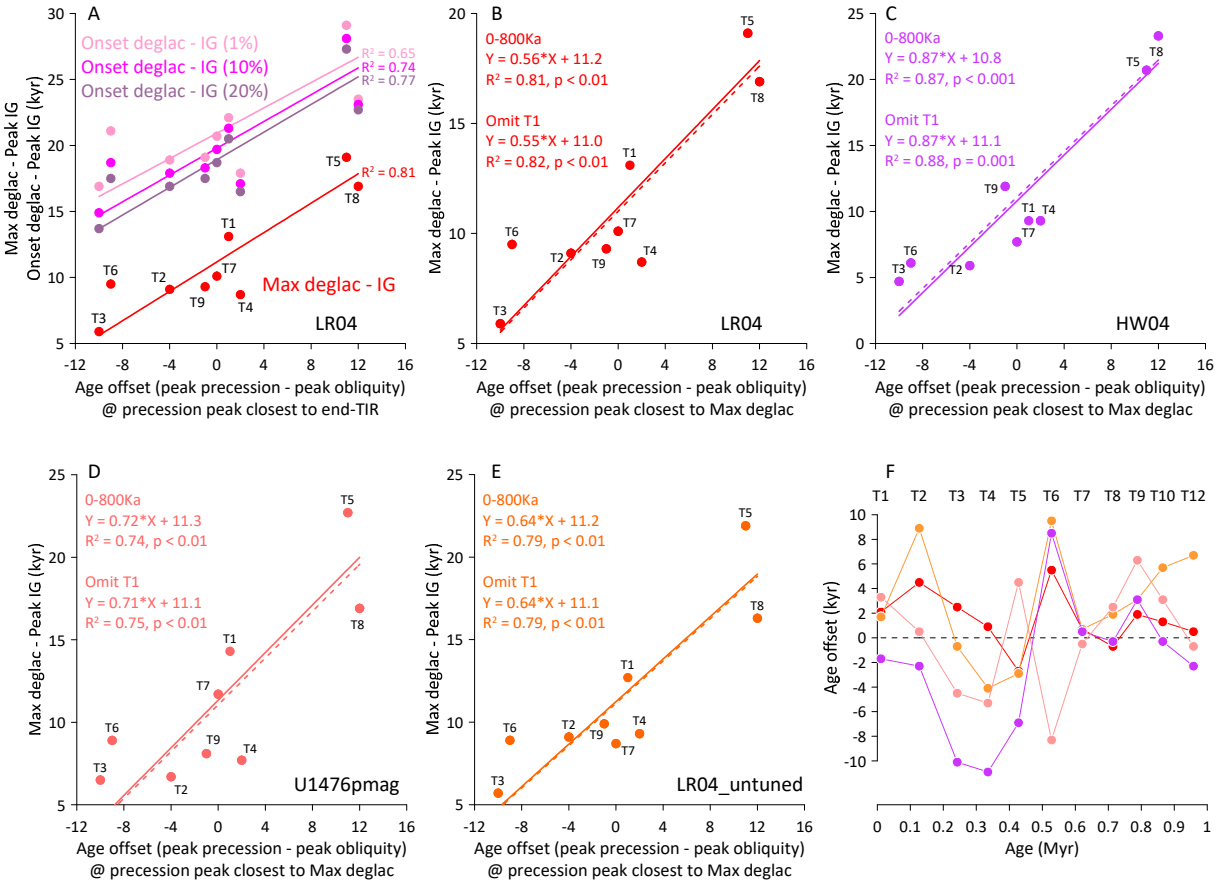

Fig. S3. Correlations between deglacial duration and the phasing of precession versus obliquity. (A) Comparison of Onset deglaciation minus Peak IG age (i.e. 'full width' of deglaciation) beginning at 1, 10 and 20% of max rate of deglaciation (see text) with Max deglac minus Peak IG age. The relatively constant offset between Onset deglac minus Peak IG and Max deglac minus Peak IG (see also Fig. 1) reflects the fact that most of the variability in the duration of deglacials involves the latter half of deglaciation (i.e. between Max deglac and Peak IG). (B-E) Max deglac minus Peak IG age versus precession minus obliquity for 3 records/stacks of benthic $\delta^{18}O$ on 4 independent age models. (F) Age offsets between Max deglac and peak precession for each record over past 1Myr. Age offsets between individual age models may be up to 18kyr but the same precession peaks are selected for each termination for all records (see also Fig. S2).

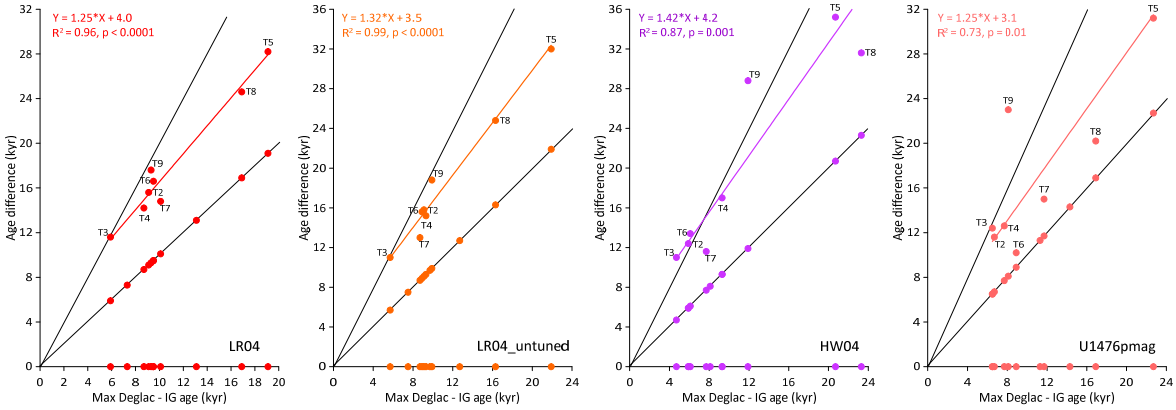

Fig. S4. Variations in interglacial duration are dominated by the deglacial interval. Correlations between Max deglac minus Max inception versus Max deglac minus Peak IG for each of the benthic $\delta^{18}O$ records/stacks analysed in this study (see also Fig. 2).

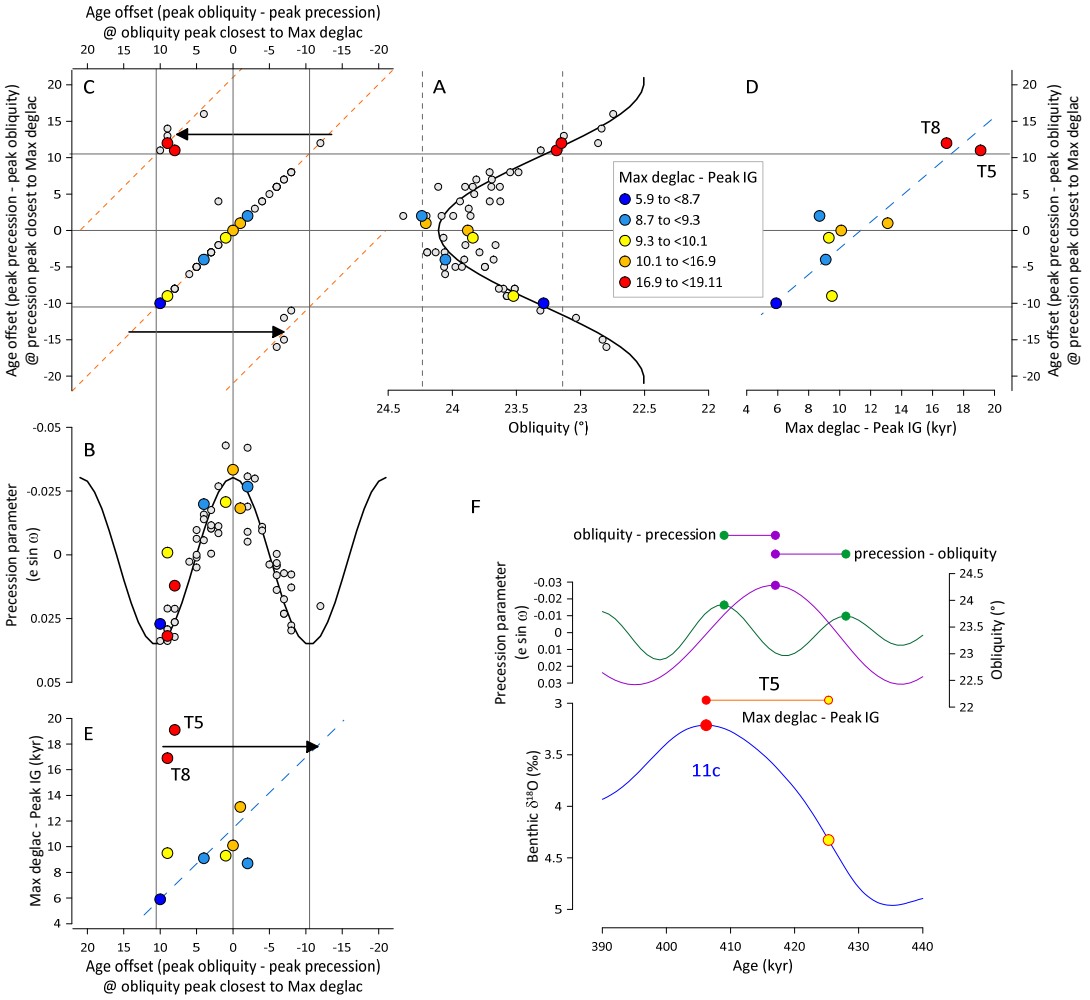

Fig. S5. Precession-minus-obliquity versus obliquity-minus-precession. (A) Value of obliquity at the precession peaks closest to all deglacial transitions in LR04 over the past 2Myr versus the peak-to-peak offset between precession and obliquity (i.e. precession-obliquity). Coloured symbols (coloured according to the respective offset between Max deglac and Peak IG) correspond to major terminations of the past 0.8Myr. (B) Same as (A) but this time symbols represent value of precession at the obliquity peaks closest to all deglacial transitions versus the peak-to-peak offset between obliquity and precession (i.e. obliquity-precession). Note reduced range of obliquity-precession in (B) compared with precession-obliquity in (A) due to the fact that the closest precession peak can be no further than 10.5kyr from a given peak in obliquity while the closest obliquity peak can be up to 20.5kyr from a given peak in precession. (C) This results in an incorrect obliquity-precession offset being assigned to particularly long deglaciations (e.g. T5 in part (F)) where the nearest precession peak to the closest obliquity peak to Max deglac is not the same as the closest precession peak to Max deglac. The resulting correlation between Max deglac-Peak IG and obliquity-precession (E) is truncated when compared with that between Max deglac-Peak IG and precession-obliquity (D).

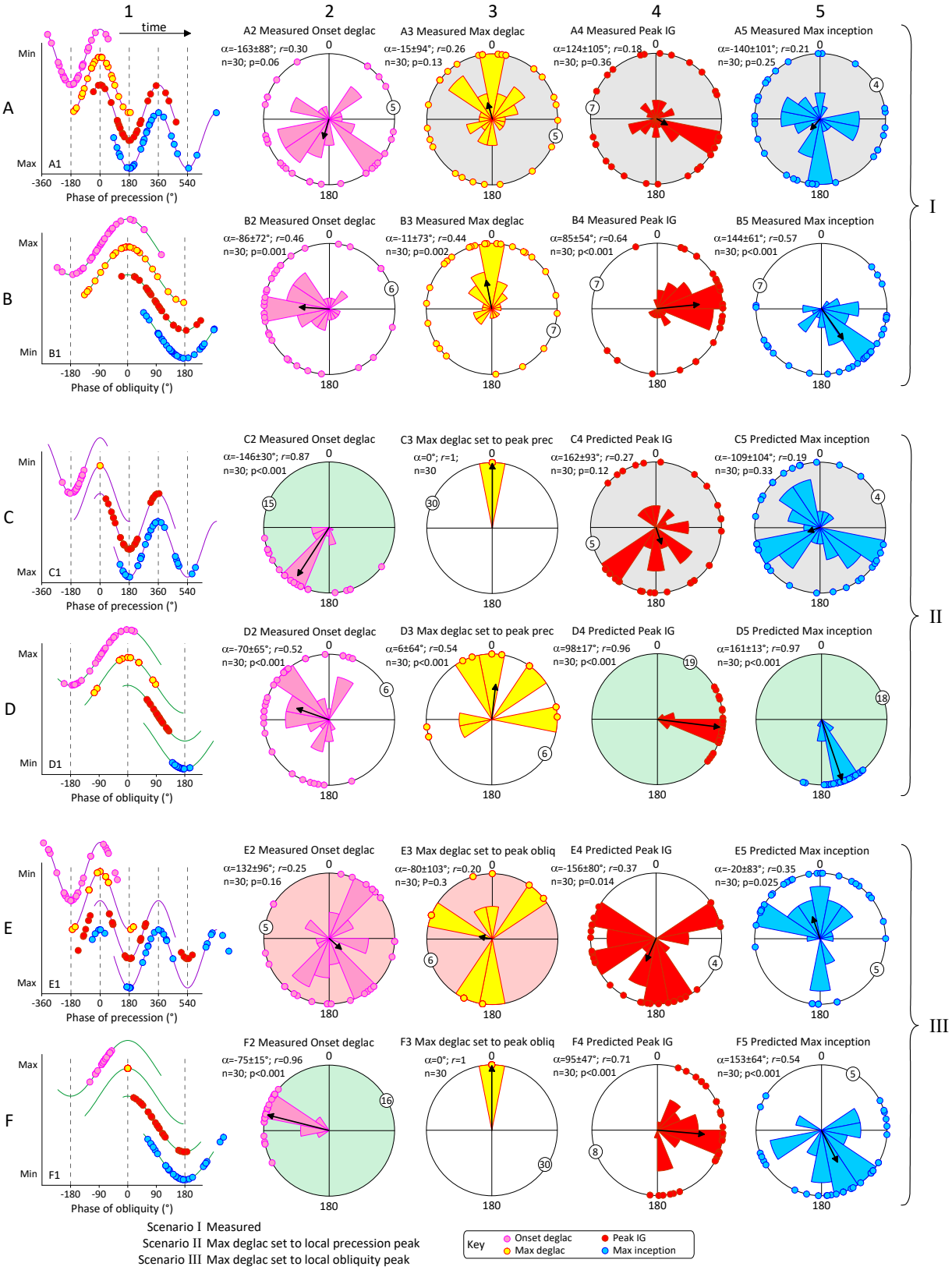
1
2
3
4
5
time
A
B
C
D
E
F
Min
Max
A1
B1
C1
D1
E1
F1
-360 -180 0 180 360 540
Phase of precession (°)
-180 -90 0 90 180
Phase of obliquity (°)
A2 Measured Onset deglac
α=-163±88°; r=0.30
n=30; p=0.06
A3 Measured Max deglac
α=-15±94°; r=0.26
n=30; p=0.13
A4 Measured Peak IG
α=124±105°; r=0.18
n=30; p=0.36
A5 Measured Max inception
α=-140±101°; r=0.21
n=30; p=0.25
B2 Measured Onset deglac
α=-86±72°; r=0.46
n=30; p=0.001
B3 Measured Max deglac
α=-11±73°; r=0.44
n=30; p=0.002
B4 Measured Peak IG
α=85±54°; r=0.64
n=30; p<0.001
B5 Measured Max inception
α=144±61°; r=0.57
n=30; p<0.001
C2 Measured Onset deglac
α=-146±30°; r=0.87
n=30; p<0.001
C3 Max deglac set to peak prec
α=0°; r=1;
n=30
C4 Predicted Peak IG
α=162±93°; r=0.27
n=30; p=0.12
C5 Predicted Max inception
α=-109±104°; r=0.19
n=30; p=0.33
D2 Measured Onset deglac
α=-70±65°; r=0.52
n=30; p<0.001
D3 Max deglac set to peak prec
α=6±64°; r=0.54
n=30; p<0.001
D4 Predicted Peak IG
α=98±17°; r=0.96
n=30; p<0.001
D5 Predicted Max inception
α=161±13°; r=0.97
n=30; p<0.001
E2 Measured Onset deglac
α=132±96°; r=0.25
n=30; p=0.16
E3 Max deglac set to peak obliq
α=-80±103°; r=0.20
n=30; P=0.3
E4 Predicted Peak IG
α=-156±80°; r=0.37
n=30; p=0.014
E5 Predicted Max inception
α=-20±83°; r=0.35
n=30; p=0.025
F2 Measured Onset deglac
α=-75±15°; r=0.96
n=30; p<0.001
F3 Max deglac set to peak obliq
α=0°; r=1
n=30
F4 Predicted Peak IG
α=95±47°; r=0.71
n=30; p<0.001
F5 Predicted Max inception
α=153±64°; r=0.54
n=30; p<0.001
0
180
I
II
III
Scenario I Measured
Scenario II Max deglac set to local precession peak
Scenario III Max deglac set to local obliquity peak
Key
Onset deglac
Max deglac
Peak IG
Max inception

Fig. S6. Precession determines the onset of deglaciation. Results for LR04_untuned, HW04 and U1476pmag from Scenarios I-III in Section 4 (see also Table S2). Column (1) (repeated from Fig. 4) timing of Onset deglac, Max deglac, Peak IG and Max inception with respect to the phase of precession and obliquity for Terminations T2 to T12. In each case, zero phase is the closest precession/obliquity peak to Max deglac. Columns (2-5) represent the same results using rose diagrams to illustrate the relative phasing for individual records. In each case α is the mean direction $\pm 1\sigma$ for all events, r is length of the mean resultant vector ($r \rightarrow 1$ as data converge; see Methods). Black arrow is the mean resultant vector (angle = α, length = r * radial axis). Circled number is length of radial axis. In Scenario I (rows A, B) each event is derived directly from the published records on their respective age models. In Scenario II (rows C, D) Max deglac is set to the nearest precession peak (C3). Offsets from Onset deglac to Max deglac are measured (C2, D2) while Max deglac to Peak IG (C4, D4) and Max inception (C5, D5) are predicted from relationships in Figs 2, S3. In Scenario III (rows E, F) Max deglac is set to the nearest obliquity peak (F3). Grey shading indicates $p>0.1$, pink shading indicates $p>0.1$ with respect to Scenario I (i.e. alignment is significantly worse), green shading indicates $r > 0.8$ and $r > 0.1$ with respect to Scenario I (i.e. alignment is significantly stronger).

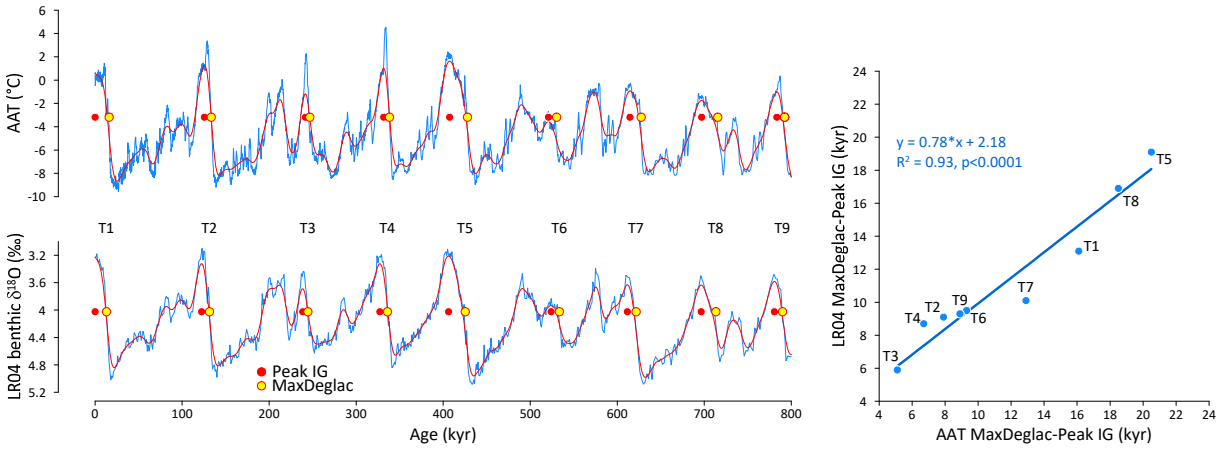

Fig. S7. Morphological similarity of Antarctic temperature and LR04 benthic $\delta^{18}O$ stack. Close agreement between the shape of AAT (in this case the stacked record of Parrenin et al., (*44*) on the AICC2012 timescale (*86, 87*)) and LR04 implies a common control across deglaciation. Pre-treatment (i.e. smoothing and differentiating) of AAT was identical to that described for LR04 in Methods.

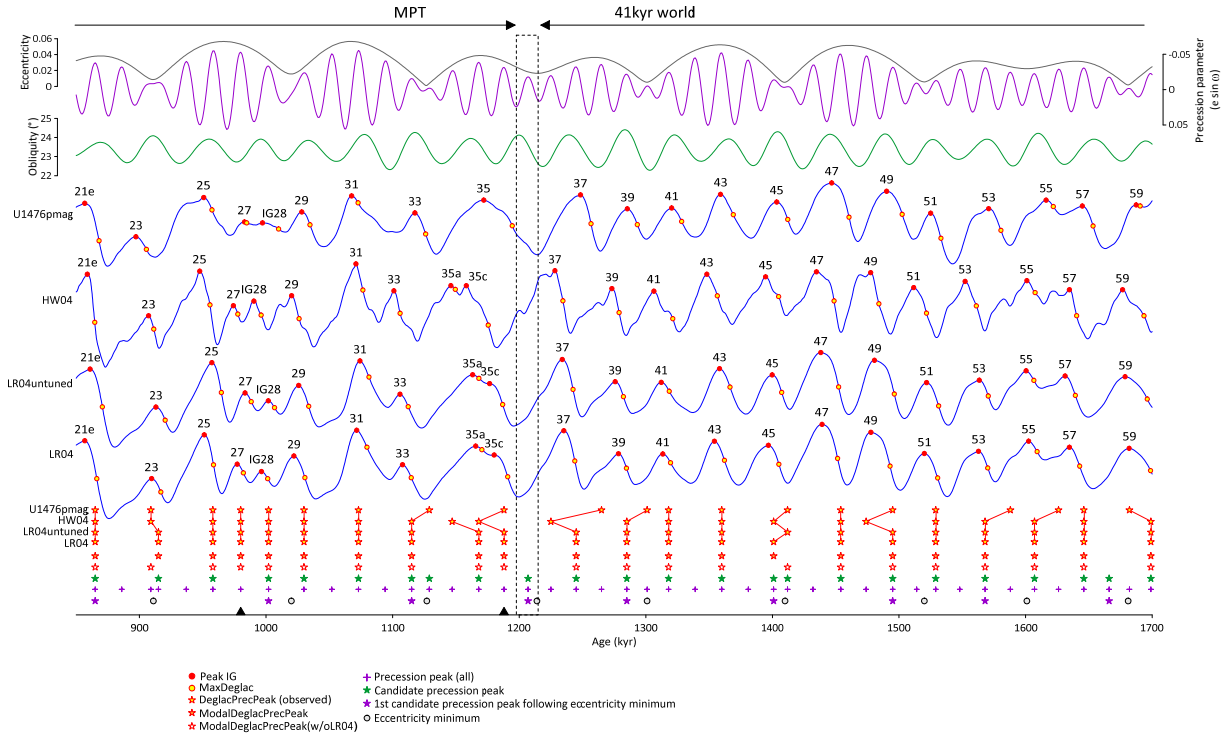

Fig. S8. Deglaciations of the 41kyr world and MPT. Prior to the MPT deglacial transitions were more closely aligned with candidate precession peaks (i.e. those that commenced while obliquity was increasing) than with non-candidate peaks, with almost all candidate peaks being associated with a deglacial event. This resulted in glacial periods being roughly equal in length to the period of obliquity, and implies no (significant) influence of eccentricity on glacial periods prior to the MPT. A similar situation is observed during the MPT except that deglacial events were also (occasionally) aligned with non-candidate precession peaks (indicated by black triangles). The first of these events (the deglaciation leading into MIS 35c) followed the first instance of a rise in obliquity not being associated with deglaciation (dotted rectangle). As noted previously (*11*) the subsequent fall in obliquity was the only instance during the past 1.7Myr when a minimum in obliquity was not associated with the onset or continuation of significant ice rafting across the North Atlantic. The interval highlighted by the dotted rectangle can therefore be considered as the definitive end of the 41kyr world. 'DeglacPrecPeak (observed)' = nearest precession peak to MaxDeglac for each stack/record of benthic $\delta^{18}O$; 'ModalDeglacPrecPeak' = average (modal) precession peak for the various records on 4 independent age models (where no mode exists the peak closest to the mean age is selected); 'ModalDeglacPrecPeak(w/oLR04)' = same, but not including LR04.

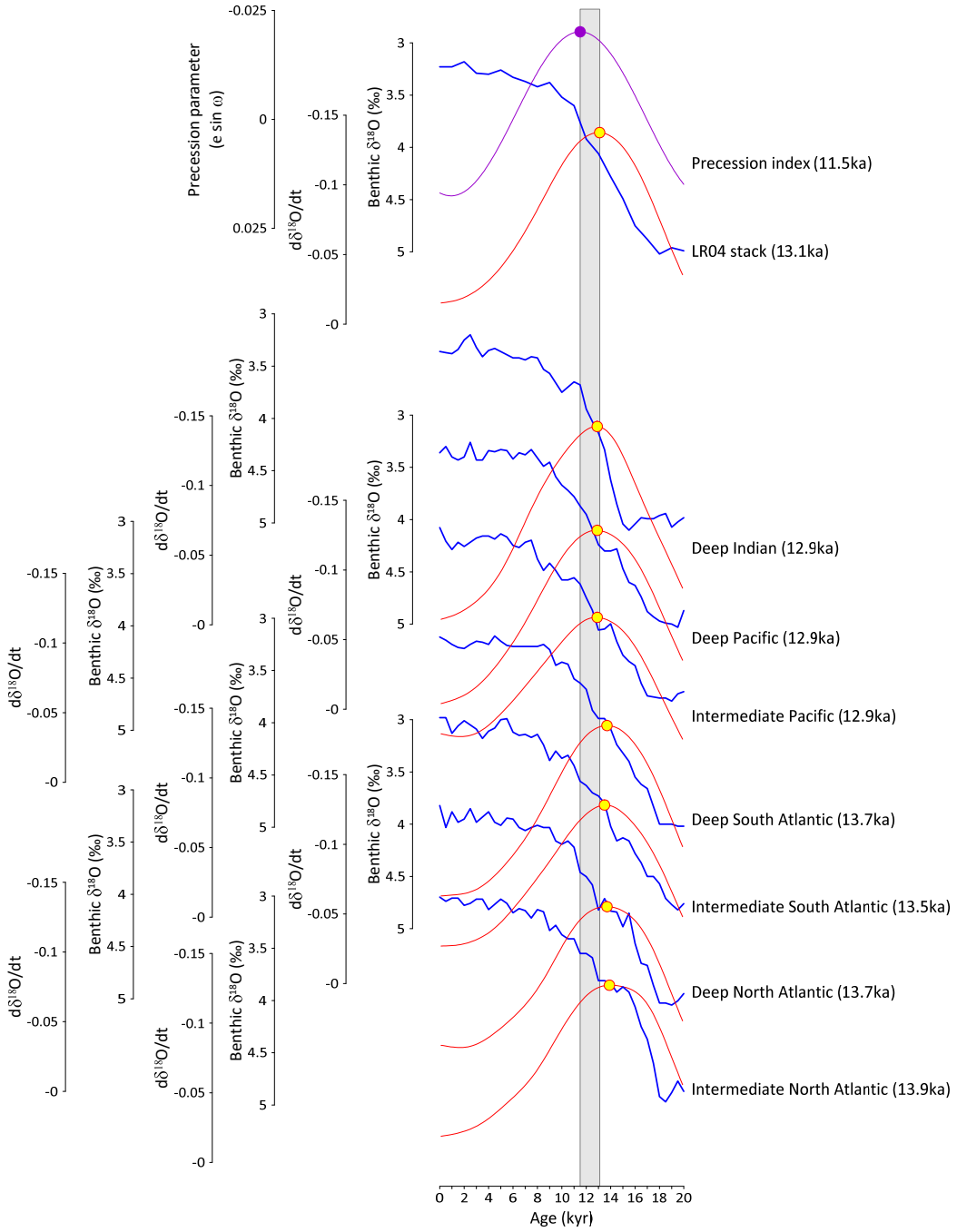

Fig. S9. Timing of Max deglaciation across Termination 1 (T1) versus peak (minimum) precession. Uppermost curve is precession parameter with peak highlighted by purple symbol. Also plotted at top is the LR04 benthic $\delta^{18}O$ stack along with its rate of change (Max deglac is highlighted by yellow symbol). According to the LR04 age model Max deglac occurred ~13.1ka, 1.6kyr before the peak in precession. Other curves show results for regional benthic $\delta^{18}O$ stacks as derived by Stern and Lisiecki (*81*). Grey box spans age estimates for peak precession and LR04 stack. These results suggest that Max deglac can be assumed to align with a minimum in precession with an uncertainty of ~2.5kyr.

						Termination 1			Termination 5		
							Calculated (predicted)			Calculated (predicted)	
	Smooth (kyr)	A	B	n	R^2	Prec-Obl (kyr)	MaxDeglac-Peak IG (kyr)	1σ	Prec-Obl (kyr)	MaxDeglac-Peak IG (kyr)	1σ
LR04	7	0.632	11.17	8	0.78	2	12.4		11	18.1	
	8	0.597	11.12	8	0.80	2	12.3		11	17.7	
	9	0.550	11.01	8	0.81	2	12.1		11	17.1	
	10	0.513	11.01	8	0.80	2	12.0		11	16.7	
	11	0.473	11.04	8	0.80	2	12.0		11	16.2	
	12	0.430	11.17	8	0.78	2	12.0		11	15.9	
							12.2	0.2		16.9	0.9
Luntuned04	7	0.723	11.41	8	0.77	2	12.9		11	19.4	
	8	0.693	11.34	8	0.78	2	12.7		11	19.0	
	9	0.641	11.14	8	0.79	2	12.4		11	18.2	
	10	0.598	11.13	8	0.79	2	12.3		11	17.7	
	11	0.555	11.26	8	0.77	2	12.4		11	17.4	
	12	0.504	11.41	8	0.74	2	12.4		11	17.0	
							12.5	0.2		18.1	0.9
HW04	1	0.865	11.09	8	0.88	2	12.8		11	20.6	
	2	0.855	10.94	8	0.87	2	12.7		11	20.3	
	3	0.853	11.02	8	0.87	2	12.7		11	20.4	
	4	0.834	11.10	8	0.87	2	12.8		11	20.3	
	5	0.810	11.20	8	0.87	2	12.8		11	20.1	
	6	0.783	11.33	8	0.87	2	12.9		11	19.9	
							12.8	0.1		20.3	0.2
U1476pmag	7	0.772	10.08	8	0.77	2	11.6		11	18.6	
	8	0.747	10.71	8	0.79	2	12.2		11	18.9	
	9	0.709	11.06	8	0.75	2	12.5		11	18.9	
	10	0.638	11.47	8	0.74	2	12.7		11	18.5	
	11	0.701	11.27	7	0.83	2	12.7		11	19.0	
	12	0.704	11.29	7	0.79	2	12.7		11	19.0	
							12.4	0.4		18.8	0.2

Table S1. Effect of smoothing window (applied to benthic $\delta^{18}O$ records/stacks before differentiating) on RMA linear fits of MaxDeglac-Peak IG versus precession-obliquity (MaxDeglac-Peak IG = Ax+B, where x = precession-obliquity) (Fig. S3). Fits are based on T2-9 (i.e. excluding T1). The difference in calculated MaxDeglac-Peak IG is minimal for low peak-to-peak offsets (e.g. T1), rising to several hundred years for larger offsets, depending on the record employed. The smoothing window used for the final calculations in each case is indicated by green shading.

Scenario I: Measured

1.1. Relative to local precession peak (Fig. S6A)

	Onset Deglac					Max Deglac					Peak IG					Max inception				
	n	p value	*r*	Angle	1σ	n	p value	*r*	Angle	1σ	n	p value	*r*	Angle	1σ	n	p value	*r*	Angle	1σ
LR04	10	0.01	0.68	-169	51	10	0.00	0.79	-24	39	10	0.04	0.56	99	62	10	0.16	0.43	-153	75
LuntunedR04	10	0.44	0.29	-180	90	10	0.41	0.30	-49	89	10	0.41	0.30	67	89	10	0.44	0.29	-179	90
HW04	10	0.56	0.24	-108	96	10	0.66	0.21	24	102	10	0.37	0.32	121	87	10	0.83	0.14	171	114
U1476pmag	10	0.08	0.50	-177	67	10	0.27	0.37	-10	81	10	0.47	0.28	-160	91	10	0.15	0.43	-99	74
All events	**40**	**0.00**	**0.40**	**-166**	**78**	**40**	**0.00**	**0.39**	**-20**	**78**	**40**	**0.05**	**0.27**	**112**	**92**	**40**	**0.06**	**0.27**	**-145**	**93**
All events w/o LR04	**30**	**0.06**	**0.30**	**-163**	**88**	**30**	**0.13**	**0.26**	**-15**	**94**	**30**	**0.36**	**0.18**	**124**	**105**	**30**	**0.25**	**0.21**	**-140**	**101**

1.2. Relative to local obliquity peak (Fig. S6B)

	Onset Deglac					Max Deglac					Peak IG					Max inception				
	n	p value	*r*	Angle	1σ	n	p value	*r*	Angle	1σ	n	p value	*r*	Angle	1σ	n	p value	*r*	Angle	1σ
LR04	10	0.00	0.77	-86	41	10	0.00	0.72	-11	46	10	0.00	0.89	80	28	10	0.00	0.80	146	38
LuntunedR04	10	0.01	0.68	-105	50	10	0.02	0.61	-28	57	10	0.00	0.73	70	46	10	0.00	0.75	127	44
HW04	10	0.05	0.54	-61	63	10	0.07	0.51	5	67	10	0.00	0.71	103	48	10	0.08	0.50	177	68
U1476pmag	10	0.59	0.23	-92	98	10	0.54	0.25	-2	95	10	0.05	0.54	82	64	10	0.03	0.58	139	60
All events	**40**	**0.00**	**0.54**	**-86**	**64**	**40**	**0.00**	**0.51**	**-11**	**66**	**40**	**0.00**	**0.70**	**83**	**48**	**40**	**0.00**	**0.63**	**145**	**55**
All events w/o LR04	**30**	**0.00**	**0.46**	**-86**	**72**	**30**	**0.00**	**0.44**	**-11**	**73**	**30**	**0.00**	**0.64**	**85**	**54**	**30**	**0.00**	**0.57**	**144**	**61**

Scenario II: Max deglac set to closest precession peak

2.1. Relative to local precession peak

2.1.1. Measured offsets

	Onset Deglac					Max Deglac					Peak IG					Max inception				
	n	p value	*r*	Angle	1σ	n	p value	*r*	Angle	1σ	n	p value	*r*	Angle	1σ	n	p value	*r*	Angle	1σ
LR04	10	0.00	0.94	-145	20			1	0		10	0.04	0.57	156	61	10	0.30	0.35	-93	83
LuntunedR04	10	0.00	0.94	-144	20			1	0		10	0.02	0.61	148	57	10	0.04	0.56	-110	62
HW04	10	0.00	0.97	-131	14			1	0		10	0.02	0.61	109	57	10	0.00	0.79	-149	40
U1476pmag	10	0.00	0.81	-169	38			1	0		10	0.04	0.55	139	63	10	0.08	0.50	-152	67
All events	**40**	**0.00**	**0.89**	**-146**	**28**			**1**	**0**		**40**	**0.00**	**0.56**	**138**	**62**	**40**	**0.00**	**0.50**	**-131**	**67**
All events w/o LR04	**30**	**0.00**	**0.87**	**-146**	**30**			**1**	**0**		**30**	**0.00**	**0.56**	**132**	**61**	**30**	**0.00**	**0.58**	**-138**	**59**

2.1.2. Measured/Predicted offsets (Fig. S6C)

LR04	"	"	"	"	"			"	"		10	0.11	0.47	-177	70	10	0.42	0.30	-75	89
LuntunedR04	"	"	"	"	"			"	"		10	0.27	0.37	176	81	10	0.66	0.21	-100	102
HW04	"	"	"	"	"			"	"		10	0.68	0.20	126	103	10	0.70	0.19	-97	104
U1476pmag	"	"	"	"	"			"	"		10	0.47	0.28	167	91	10	0.69	0.20	-130	103
All events	"	"	"	"	"			"	"		**40**	**0.02**	**0.31**	**170**	**88**	**40**	**0.17**	**0.21**	**-97**	**101**
All events w/o LR04	"	"	"	"	"			"	"		**30**	**0.12**	**0.27**	**162**	**93**	**30**	**0.33**	**0.19**	**-109**	**104**

2.2. Relative to local obliquity peak

2.2.1. Measured offsets

	Onset Deglac					Max Deglac					Peak IG					Max inception				
	n	p value	*r*	Angle	1σ	n	p value	*r*	Angle	1σ	n	p value	*r*	Angle	1σ	n	p value	*r*	Angle	1σ
LR04	10	0.02	0.60	-69	58	10	0.05	0.54	6	64	10	0.00	0.78	92	40	10	0.00	0.72	158	46
LuntunedR04	10	0.02	0.60	-69	58	10	0.05	0.54	6	64	10	0.00	0.80	94	39	10	0.00	0.83	155	35
HW04	10	0.05	0.55	-62	63	10	0.05	0.54	6	64	10	0.00	0.89	91	27	10	0.01	0.68	161	51
U1476pmag	10	0.15	0.44	-81	73	10	0.05	0.54	6	64	10	0.00	0.76	94	43	10	0.01	0.66	143	52
All events	**40**	**0.00**	**0.54**	**-70**	**63**	**40**	**0.00**	**0.54**	**6**	**64**	**40**	**0.00**	**0.81**	**93**	**37**	**40**	**0.00**	**0.72**	**154**	**47**
All events w/o LR04	**30**	**0.00**	**0.52**	**-70**	**65**	**30**	**0.00**	**0.54**	**6**	**64**	**30**	**0.00**	**0.82**	**93**	**37**	**30**	**0.00**	**0.72**	**153**	**47**

2.2.2. Measured/Predicted offsets (Fig. S6D)

LR04	"	"	"	"	"	"	"	"	"	"	10	0.00	0.89	99	27	10	0.00	0.95	158	19
LuntunedR04	"	"	"	"	"	"	"	"	"	"	10	0.00	0.93	99	22	10	0.00	0.99	161	10
HW04	"	"	"	"	"	"	"	"	"	"	10	0.00	0.99	95	8	10	0.00	0.97	171	15
U1476pmag	"	"	"	"	"	"	"	"	"	"	10	0.00	0.96	99	17	10	0.00	0.99	151	6
All events	"	"	"	"	"	"	"	"	"	"	**40**	**0.00**	**0.94**	**98**	**20**	**40**	**0.00**	**0.97**	**160**	**15**
All events w/o LR04	"	"	"	"	"	"	"	"	"	"	**30**	**0.00**	**0.96**	**98**	**17**	**30**	**0.00**	**0.97**	**161**	**13**

Scenario III: Max deglac set to closest obliquity peak

3.1. Relative to local precession peak

3.1.1. Measured offsets

	Onset Deglac					Max Deglac					Peak IG					Max inception				
	n	p value	*r*	Angle	1σ	n	p value	*r*	Angle	1σ	n	p value	*r*	Angle	1σ	n	p value	*r*	Angle	1σ
LR04	10	0.62	0.22	119	99	10	0.68	0.20	-80	103	10	0.07	0.51	143	66	10	0.09	0.49	-68	69
LuntunedR04	10	0.61	0.23	124	99	10	0.68	0.20	-80	103	10	0.13	0.46	152	72	10	0.62	0.22	-65	99
HW04	10	0.65	0.21	136	101	10	0.68	0.20	-80	103	10	0.40	0.31	-152	88	10	0.39	0.31	78	87
U1476pmag	10	0.40	0.31	135	88	10	0.68	0.20	-80	103	10	0.26	0.37	152	81	10	0.97	0.05	-147	140
All events	**40**	**0.10**	**0.24**	**129**	**97**	**40**	**0.20**	**0.20**	**-80**	**103**	**40**	**0.00**	**0.38**	**159**	**80**	**40**	**0.56**	**0.12**	**-51**	**118**
All events w/o LR04	**30**	**0.16**	**0.25**	**132**	**96**	**30**	**0.30**	**0.20**	**-80**	**103**	**30**	**0.03**	**0.34**	**166**	**84**	**30**	**0.94**	**0.05**	**33**	**142**

3.1.2. Measured/Predicted offsets (Fig. S6E)

LR04	"	"	"	"	"	"	"	"	"	"	10	0.48	0.27	-173	92	10	0.28	0.36	-41	82
LuntunedR04	"	"	"	"	"	"	"	"	"	"	10	0.36	0.32	-163	86	10	0.17	0.42	-25	75
HW04	"	"	"	"	"	"	"	"	"	"	10	0.16	0.43	-152	75	10	0.44	0.29	21	90
U1476pmag	"	"	"	"	"	"	"	"	"	"	10	0.26	0.37	-154	81	10	0.16	0.43	-40	74
All events	"	"	"	"	"	"	"	"	"	"	**40**	**0.01**	**0.35**	**-159**	**84**	**40**	**0.01**	**0.35**	**-25**	**83**
All events w/o LR04	"	"	"	"	"	"	"	"	"	"	**30**	**0.01**	**0.37**	**-156**	**80**	**30**	**0.03**	**0.35**	**-20**	**83**

3.2. Relative to local obliquity peak

3.2.1. Measured offsets

	Onset Deglac					Max Deglac					Peak IG					Max inception				
	n	p value	*r*	Angle	1σ	n	p value	*r*	Angle	1σ	n	p value	*r*	Angle	1σ	n	p value	*r*	Angle	1σ
LR04	10	0.00	0.98	-74	10			1	0		10	0.00	0.84	90	34	10	0.00	0.73	157	45
LuntunedR04	10	0.00	0.98	-73	10			1	0		10	0.00	0.80	89	38	10	0.01	0.69	144	50
HW04	10	0.00	0.99	-67	7			1	0		10	0.01	0.65	79	53	10	0.19	0.41	123	77
U1476pmag	10	0.00	0.95	-87	19			1	0		10	0.00	0.75	87	43	10	0.01	0.63	126	55
All events	**40**	**0.00**	**0.97**	**-75**	**14**			**1**	**0**		**40**	**0.00**	**0.76**	**87**	**43**	**40**	**0.00**	**0.60**	**140**	**58**
All events	**30**	**0.00**	**0.96**	**-75**	**15**			**1**	**0**		**30**	**0.00**	**0.73**	**85**	**45**	**30**	**0.00**	**0.57**	**133**	**61**

3.2.2. Measured/Predicted offsets (Fig. S6F)

LR04	"	"	"	"	"			"	"		10	0.00	0.83	98	35	10	0.00	0.74	156	44
LuntunedR04	"	"	"	"	"			"	"		10	0.00	0.78	97	40	10	0.01	0.65	157	54
HW04	"	"	"	"	"			"	"		10	0.02	0.63	91	55	10	0.25	0.37	157	80
U1476pmag	"	"	"	"	"			"	"		10	0.00	0.73	97	45	10	0.02	0.61	147	57
All events	"	"	"	"	"			"	"		**40**	**0.00**	**0.74**	**96**	**44**	**40**	**0.00**	**0.59**	**154**	**59**
All events	"	"	"	"	"			"	"		**30**	**0.00**	**0.71**	**95**	**47**	**30**	**0.00**	**0.54**	**153**	**64**

p > 0.1	p > 0.1 wrt measured
p > 0.05	*r* > 0.8 & *r* > 0.1 wrt measured

Table S2. Results for Scenarios I-III for individual benthic $\delta^{18}O$ records and combinations with and without LR04. Scenario I: All points are obtained directly from records on their original

timescales. Scenario II: Max deglac is set to the nearest precession peak. Scenario III: Max deglac is set to the nearest obliquity peak. In Scenarios II and III, measured offsets (relative to Max deglac) are obtained from the original records; predicted offsets are obtained from the relationships shown in Figures 2, S3, S4. Colour-coding is same as used in Figure S6

References and Notes

1. J. D. Hays, J. Imbrie, N. J. Shackleton, Variations in the Earth's Orbit: Pacemaker of the Ice Ages. *Science* **194**, 1121–1132 (1976). doi:10.1126/science.194.4270.1121 Medline

2. M. E. Raymo, The timing of major climate terminations. *Paleoceanography* **12**, 577–585 (1997). doi:10.1029/97PA01169

3. A. J. Ridgwell, A. J. Watson, M. E. Raymo, Is the spectral signature of the 100 kyr glacial cycle consistent with a Milankovitch origin? *Paleoceanography* **14**, 437–440 (1999). doi:10.1029/1999PA900018

4. H. Cheng, R. L. Edwards, A. Sinha, C. Spötl, L. Yi, S. Chen, M. Kelly, G. Kathayat, X. Wang, X. Li, X. Kong, Y. Wang, Y. Ning, H. Zhang, The Asian monsoon over the past 640,000 years and ice age terminations. *Nature* **534**, 640–646 (2016). doi:10.1038/nature18591 Medline

5. B. Hobart, L. E. Lisiecki, D. Rand, T. Lee, C. E. Lawrence, Late Pleistocene 100-kyr glacial cycles paced by precession forcing of summer insolation. *Nat. Geosci.* **16**, 717–722 (2023). doi:10.1038/s41561-023-01235-x

6. P. Huybers, C. Wunsch, Obliquity pacing of the late Pleistocene glacial terminations. *Nature* **434**, 491–494 (2005). doi:10.1038/nature03401 Medline

7. P. Bajo, R. N. Drysdale, J. D. Woodhead, J. C. Hellstrom, D. Hodell, P. Ferretti, A. H. L. Voelker, G. Zanchetta, T. Rodrigues, E. Wolff, J. Tyler, S. Frisia, C. Spötl, A. E. Fallick, Persistent influence of obliquity on ice age terminations since the Middle Pleistocene transition. *Science* **367**, 1235–1239 (2020). doi:10.1126/science.aaw1114 Medline

8. P. Huybers, Combined obliquity and precession pacing of late Pleistocene deglaciations. *Nature* **480**, 229–232 (2011). doi:10.1038/nature10626 Medline

9. F. Parrenin, D. Paillard, Terminations VI and VIII (~530 and ~720 kyr BP) tell us the importance of obliquity and precession in the triggering of deglaciations. *Clim. Past* **8**, 2031–2037 (2012). doi:10.5194/cp-8-2031-2012

10. P. C. Tzedakis, M. Crucifix, T. Mitsui, E. W. Wolff, A simple rule to determine which insolation cycles lead to interglacials. *Nature* **542**, 427–432 (2017). doi:10.1038/nature21364 Medline

11. S. Barker, A. Starr, J. van der Lubbe, A. Doughty, G. Knorr, S. Conn, S. Lordsmith, L. Owen, A. Nederbragt, S. Hemming, I. Hall, L. Levay, IODP Exp 361 Shipboard Scientific Party, Persistent influence of precession on northern ice sheet variability since the early Pleistocene. *Science* **376**, 961–967 (2022). doi:10.1126/science.abm4033 Medline

12. J. Imbrie, A. Berger, E. A. Boyle, S. C. Clemens, A. Duffy, W. R. Howard, G. Kukla, J. Kutzbach, D. G. Martinson, A. McIntyre, A. C. Mix, B. Molfino, J. J. Morley, L. C. Peterson, N. G. Pisias, W. L. Prell, M. E. Raymo, N. J. Shackleton, J. R. Toggweiler, On the structure and origin of major glaciation cycles 2. The 100,000-year cycle. *Paleoceanography* **8**, 699–735 (1993). doi:10.1029/93PA02751

13. A. Ganopolski, Toward generalized Milankovitch theory (GMT). *Clim. Past* **20**, 151–185 (2024). doi:10.5194/cp-20-151-2024

14. L. E. Lisiecki, Links between eccentricity forcing and the 100,000-year glacial cycle. *Nat. Geosci.* **3**, 349–352 (2010). doi:10.1038/ngeo828

15. H. Elderfield, P. Ferretti, M. Greaves, S. Crowhurst, I. N. McCave, D. Hodell, A. M. Piotrowski, Evolution of ocean temperature and ice volume through the mid-Pleistocene climate transition. *Science* **337**, 704–709 (2012). doi:10.1126/science.1221294 Medline

16. See the Materials and methods section.

17. D. Baggenstos, M. Häberli, J. Schmitt, S. A. Shackleton, B. Birner, J. P. Severinghaus, T. Kellerhals, H. Fischer, Earth's radiative imbalance from the Last Glacial Maximum to the present. *Proc. Natl. Acad. Sci. U.S.A.* **116**, 14881–14886 (2019). doi:10.1073/pnas.1905447116 Medline

18. S. Shackleton, A. Seltzer, D. Baggenstos, L. E. Lisiecki, Benthic $\delta^{18}O$ records Earth's energy imbalance. *Nat. Geosci.* **16**, 797–802 (2023). doi:10.1038/s41561-023-01250-y

19. L. E. Lisiecki, M. E. Raymo, A Pliocene-Pleistocene stack of 57 globally distributed benthic $\delta^{18}O$ records. *Paleoceanography* **20**, PA1003 (2005). doi:10.1029/2004PA001071

20. P. Huybers, C. Wunsch, A depth-derived Pleistocene age model: Uncertainty estimates, sedimentation variability, and nonlinear climate change. *Paleoceanography* **19**, PA1028 (2004). doi:10.1029/2002PA000857

21. P. Huybers, Glacial variability over the last two million years: An extended depth-derived agemodel, continuous obliquity pacing, and the Pleistocene progression. *Quat. Sci. Rev.* **26**, 37–55 (2007). doi:10.1016/j.quascirev.2006.07.013

22. Past Interglacials Working Group of PAGES, Interglacials of the last 800,000 years. *Rev. Geophys.* **54**, 162–219 (2016). doi:10.1002/2015RG000482

23. G. Roe, In defense of Milankovitch. *Geophys. Res. Lett.* **33**, L24703 (2006). doi:10.1029/2006GL027817

24. N. J. Shackleton, N. D. Opdyke, Oxygen isotope and palaeomagnetic stratigraphy of Equatorial Pacific core V28-238: Oxygen isotope temperatures and ice volumes on a 10^5 year and 10^6 year scale. *Quat. Res.* **3**, 39–55 (1973). doi:10.1016/0033-5894(73)90052-5

25. P. C. Tzedakis, E. Wolff, L. Skinner, V. Brovkin, D. Hodell, J. F. McManus, D. Raynaud, Can we predict the duration of an interglacial? *Clim. Past* **8**, 1473–1485 (2012). doi:10.5194/cp-8-1473-2012

26. P. Clark, J. Clague, B. B. Curry, A. Dreimanis, S. Hicock, G. Miller, G. Berger, N. Eyles, M. Lamothe, B. Miller, R. J. Mott, R. N. Oldale, R. R. Stea, J. P. Szabo, L. H. Thorleifson, J.-S. Vincent, Initiation and development of the Laurentide and Cordilleran ice sheets following the last interglaciation. *Quat. Sci. Rev.* **12**, 79–114 (1993). doi:10.1016/0277-3791(93)90011-A

27. A. Abe-Ouchi, F. Saito, K. Kawamura, M. E. Raymo, J. Okuno, K. Takahashi, H. Blatter, Insolation-driven 100,000-year glacial cycles and hysteresis of ice-sheet volume. *Nature* **500**, 190–193 (2013). doi:10.1038/nature12374 Medline

28. G. Vettoretti, W. R. Peltier, Sensitivity of glacial inception to orbital and greenhouse gas climate forcing. *Quat. Sci. Rev.* **23**, 499–519 (2004). doi:10.1016/j.quascirev.2003.08.008

29. G. Vettoretti, W. Peltier, The impact of insolation, greenhouse gas forcing and ocean circulation changes on glacial inception. *Holocene* **21**, 803–817 (2011). doi:10.1177/0959683610394885

30. M. E. Raymo, K. H. Nisancioglu, The 41 kyr world: Milankovitch's other unsolved mystery. *Paleoceanography* **18**, 1011 (2003). doi:10.1029/2002PA000791

31. A. Ganopolski, R. Winkelmann, H. J. Schellnhuber, Critical insolation–CO_2 relation for diagnosing past and future glacial inception. *Nature* **529**, 200–203 (2016). doi:10.1038/nature16494 Medline

32. A. Berger, M. F. Loutre, An exceptionally long interglacial ahead? *Science* **297**, 1287–1288 (2002). doi:10.1126/science.1076120 Medline

33. F. Parrenin, D. Paillard, Amplitude and phase of glacial cycles from a conceptual model. *Earth Planet. Sci. Lett.* **214**, 243–250 (2003). doi:10.1016/S0012-821X(03)00363-7

34. E. Legrain, F. Parrenin, E. Capron, A gradual change is more likely to have caused the Mid-Pleistocene Transition than an abrupt event. *Commun. Earth Environ.* **4**, 90 (2023). doi:10.1038/s43247-023-00754-0

35. P. C. Tzedakis, D. A. Hodell, C. Nehrbass-Ahles, T. Mitsui, E. W. Wolff, Marine Isotope Stage 11c: An unusual interglacial. *Quat. Sci. Rev.* **284**, 107493 (2022). doi:10.1016/j.quascirev.2022.107493

36. D. R. MacAyeal, A Catastrophe Model of the Paleoclimate. *J. Glaciol.* **24**, 245–257 (1979). doi:10.3189/S0022143000014775

37. S. Barker, G. Knorr, Millennial scale feedbacks determine the shape and rapidity of glacial termination. *Nat. Commun.* **12**, 2273 (2021). doi:10.1038/s41467-021-22388-6 Medline

38. S. Barker, G. Knorr, A Systematic Role for Extreme Ocean-Atmosphere Oscillations in the Development of Glacial Conditions Since the Mid Pleistocene Transition. *Paleoceanogr. Paleoclimatol.* **38**, e2023PA004690 (2023). doi:10.1029/2023PA004690

39. G. Knorr, S. Barker, X. Zhang, G. Lohmann, X. Gong, P. Gierz, C. Stepanek, L. B. Stap, A salty deep ocean as a prerequisite for glacial termination. *Nat. Geosci.* **14**, 930–936 (2021). doi:10.1038/s41561-021-00857-3

40. S. Shackleton, J. A. Menking, E. Brook, C. Buizert, M. N. Dyonisius, V. V. Petrenko, D. Baggenstos, J. P. Severinghaus, Evolution of mean ocean temperature in Marine Isotope Stage 4. *Clim. Past* **17**, 2273–2289 (2021). doi:10.5194/cp-17-2273-2021

41. R. M. DeConto, D. Pollard, Contribution of Antarctica to past and future sea-level rise. *Nature* **531**, 591–597 (2016). doi:10.1038/nature17145 Medline

42. N. R. Golledge, R. H. Levy, R. M. McKay, C. J. Fogwill, D. A. White, A. G. Graham, J. A. Smith, C.-D. Hillenbrand, K. J. Licht, G. H. Denton, R. P. Ackert Jr., S. M. Maas, B. L. Hall, Glaciology and geological signature of the Last Glacial Maximum Antarctic ice sheet. *Quat. Sci. Rev.* **78**, 225–247 (2013). doi:10.1016/j.quascirev.2013.08.011

43. J. Jouzel, V. Masson-Delmotte, O. Cattani, G. Dreyfus, S. Falourd, G. Hoffmann, B. Minster, J. Nouet, J. M. Barnola, J. Chappellaz, H. Fischer, J. C. Gallet, S. Johnsen, M. Leuenberger, L. Loulergue, D. Luethi, H. Oerter, F. Parrenin, G. Raisbeck, D. Raynaud, A. Schilt, J. Schwander, E. Selmo, R. Souchez, R. Spahni, B. Stauffer, J. P. Steffensen,

B. Stenni, T. F. Stocker, J. L. Tison, M. Werner, E. W. Wolff, Orbital and millennial Antarctic climate variability over the past 800,000 years. *Science* **317**, 793–796 (2007). doi:10.1126/science.1141038 Medline

44. F. Parrenin, V. Masson-Delmotte, P. Köhler, D. Raynaud, D. Paillard, J. Schwander, C. Barbante, A. Landais, A. Wegner, J. Jouzel, Synchronous change of atmospheric CO_2 and Antarctic temperature during the last deglacial warming. *Science* **339**, 1060–1063 (2013). doi:10.1126/science.1226368 Medline

45. J. H. Mercer, in *Climate Processes and Climate Sensitivity*, J. E. Hansen, T. Takahashi, Eds. (American Geophysical Union, 1984), pp. 307–313.

46. T. T. Barrows, S. Juggins, P. De Deckker, E. Calvo, C. Pelejero, Long-term sea surface temperature and climate change in the Australian–New Zealand region. *Paleoceanography* **22**, PA2215 (2007). doi:10.1029/2006PA001328

47. P. Huybers, G. Denton, Antarctic temperature at orbital timescales controlled by local summer duration. *Nat. Geosci.* **1**, 787–792 (2008). doi:10.1038/ngeo311

48. S. Barker, P. Diz, M. J. Vautravers, J. Pike, G. Knorr, I. R. Hall, W. S. Broecker, Interhemispheric Atlantic seesaw response during the last deglaciation. *Nature* **457**, 1097–1102 (2009). doi:10.1038/nature07770 Medline

49. E. W. Wolff, H. Fischer, R. Rothlisberger, Glacial terminations as southern warmings without northern control. *Nat. Geosci.* **2**, 206–209 (2009). doi:10.1038/ngeo442

50. G. H. Denton, R. F. Anderson, J. R. Toggweiler, R. L. Edwards, J. M. Schaefer, A. E. Putnam, The last glacial termination. *Science* **328**, 1652–1656 (2010). doi:10.1126/science.1184119 Medline

51. C. Wunsch, Greenland–Antarctic phase relations and millennial time-scale climate fluctuations in the Greenland ice-cores. *Quat. Sci. Rev.* **22**, 1631–1646 (2003). doi:10.1016/S0277-3791(03)00152-5

52. S. Barker, G. Knorr, R. L. Edwards, F. Parrenin, A. E. Putnam, L. C. Skinner, E. Wolff, M. Ziegler, 800,000 years of abrupt climate variability. *Science* **334**, 347–351 (2011). doi:10.1126/science.1203580 Medline

53. J. D. Shakun, P. U. Clark, F. He, S. A. Marcott, A. C. Mix, Z. Liu, B. Otto-Bliesner, A. Schmittner, E. Bard, Global warming preceded by increasing carbon dioxide concentrations during the last deglaciation. *Nature* **484**, 49–54 (2012). doi:10.1038/nature10915 Medline

54. D. Paillard, The timing of Pleistocene glaciations from a simple multiple-state climate model. *Nature* **391**, 378–381 (1998). doi:10.1038/34891

55. S. Barker, G. Knorr, S. Conn, S. Lordsmith, D. Newman, D. Thornalley, Early Interglacial Legacy of Deglacial Climate Instability. *Paleoceanogr. Paleoclimatol.* **34**, 1455–1475 (2019). doi:10.1029/2019PA003661

56. N. Lang, E. W. Wolff, Interglacial and glacial variability from the last 800 ka in marine, ice and terrestrial archives. *Clim. Past* **7**, 361–380 (2011). doi:10.5194/cp-7-361-2011

57. N. J. Shackleton, N. D. Opdyke, Oxygen-isotope and paleomagnetic stratigraphy of Pacific core V28-239 late Pliocene to latest Pleistocene. *Mem. Geol. Soc. Amer.* **145**, 4498–4464 (1976).

58. N. G. Pisias, T. Moore Jr., The evolution of Pleistocene climate: A time series approach. *Earth Planet. Sci. Lett.* **52**, 450–458 (1981). doi:10.1016/0012-821X(81)90197-7

59. P. U. Clark, D. Archer, D. Pollard, J. D. Blum, J. A. Rial, V. Brovkin, A. C. Mix, N. G. Pisias, M. Roy, The middle Pleistocene transition: Characteristics. mechanisms, and implications for long-term changes in atmospheric pCO_2. *Quat. Sci. Rev.* **25**, 3150–3184 (2006). doi:10.1016/j.quascirev.2006.07.008

60. S. Barker, X. Zhang, L. Jonkers, S. Lordsmith, S. Conn, G. Knorr, Strengthening Atlantic Inflow Across the Mid-Pleistocene Transition. *Paleoceanogr. Paleoclimatol.* **36**, e2020PA004200 (2021). doi:10.1029/2020PA004200

61. P. U. Clark, D. Pollard, Origin of the middle Pleistocene transition by ice sheet erosion of regolith. *Paleoceanography* **13**, 1–9 (1998). doi:10.1029/97PA02660

62. W. H. Berger, E. Jansen, in *The Polar Oceans and Their Role in Shaping the Global Environment*, J. E. Overland, R. D. Muench, O. M. Johannessen, Eds. (American Geophysical Union, 1994), pp. 295–311.

63. E. L. McClymont, S. M. Sosdian, A. Rosell-Melé, Y. Rosenthal, Pleistocene sea-surface temperature evolution: Early cooling, delayed glacial intensification, and implications for the mid-Pleistocene climate transition. *Earth Sci. Rev.* **123**, 173–193 (2013). doi:10.1016/j.earscirev.2013.04.006

64. D. Liebrand, L. Lourens, D. Hodell, B. De Boer, R. Van de Wal, H. Pälike, Antarctic ice sheet and oceanographic response to eccentricity forcing during the early Miocene. *Clim. Past* **7**, 869–880 (2011). doi:10.5194/cp-7-869-2011

65. A. Holbourn, W. Kuhnt, K. G. Kochhann, N. Andersen, K. Sebastian Meier, Global perturbation of the carbon cycle at the onset of the Miocene Climatic Optimum. *Geology* **43**, 123–126 (2015). doi:10.1130/G36317.1

66. J. Zachos, M. Pagani, L. Sloan, E. Thomas, K. Billups, Trends, rhythms, and aberrations in global climate 65 Ma to present. *Science* **292**, 686–693 (2001). doi:10.1126/science.1059412 Medline

67. N. B. Sullivan, S. R. Meyers, R. H. Levy, R. M. McKay, N. R. Golledge, G. Cortese, Millennial-scale variability of the Antarctic ice sheet during the early Miocene. *Proc. Natl. Acad. Sci. U.S.A.* **120**, e2304152120 (2023). doi:10.1073/pnas.2304152120 Medline

68. M. Willeit, A. Ganopolski, R. Calov, V. Brovkin, Mid-Pleistocene transition in glacial cycles explained by declining CO_2 and regolith removal. *Sci. Adv.* **5**, eaav7337 (2019). doi:10.1126/sciadv.aav7337 Medline

69. S. R. Meyers, L. A. Hinnov, Northern Hemisphere glaciation and the evolution of Plio-Pleistocene climate noise. *Paleoceanography* **25**, PA3207 (2010). doi:10.1029/2009PA001834

70. P. C. Tzedakis, J. Channell, D. Hodell, H. Kleiven, L. Skinner, Determining the natural length of the current interglacial. *Nat. Geosci.* **5**, 138–141 (2012). doi:10.1038/ngeo1358

71. D. Archer, A. Ganopolski, A movable trigger: Fossil fuel CO_2 and the onset of the next glaciation. *Geochem. Geophys. Geosyst.* **6**, Q05003 (2005). doi:10.1029/2004GC000891

72. C. Waelbroeck, J. C. Duplessy, E. Michel, L. Labeyrie, D. Paillard, J. Duprat, The timing of the last deglaciation in North Atlantic climate records. *Nature* **412**, 724–727 (2001). doi:10.1038/35089060 Medline

73. N. J. Shackleton, M. A. Hall, E. Vincent, Phase relationships between millennial-scale events 64,000–24,000 years ago. *Paleoceanography* **15**, 565–569 (2000). doi:10.1029/2000PA000513

74. R. B. Alley, E. J. Brook, S. Anandakrishnan, A northern lead in the orbital band: North-south phasing of Ice-Age events. *Quat. Sci. Rev.* **21**, 431–441 (2002). doi:10.1016/S0277-3791(01)00072-5

75. A. Schmittner, O. A. Saenko, A. J. Weaver, Coupling of the hemispheres in observations and simulations of glacial climate change. *Quat. Sci. Rev.* **22**, 659–671 (2003). doi:10.1016/S0277-3791(02)00184-1

76. S. Barker, G. Knorr, Antarctic climate signature in the Greenland ice core record. *Proc. Natl. Acad. Sci. U.S.A.* **104**, 17278–17282 (2007). doi:10.1073/pnas.0708494104 Medline

77. L. C. Skinner, N. J. Shackleton, Deconstructing Terminations I and II: Revisiting the glacioeustatic paradigm based on deep-water temperature estimates. *Quat. Sci. Rev.* **25**, 3312–3321 (2006). doi:10.1016/j.quascirev.2006.07.005

78. D. M. Sigman, M. P. Hain, G. H. Haug, The polar ocean and glacial cycles in atmospheric CO_2 concentration. *Nature* **466**, 47–55 (2010). doi:10.1038/nature09149 Medline

79. J. F. Adkins, The role of deep ocean circulation in setting glacial climates. *Paleoceanography* **28**, 539–561 (2013). doi:10.1002/palo.20046

80. P. Berens, CircStat: A MATLAB toolbox for circular statistics. *J. Stat. Softw.* **31**, 1–21 (2009). doi:10.18637/jss.v031.i10

81. J. V. Stern, L. E. Lisiecki, Termination 1 timing in radiocarbon-dated regional benthic $\delta^{18}O$ stacks. *Paleoceanography* **29**, 1127–1142 (2014). doi:10.1002/2014PA002700

82. B. Bereiter, S. Shackleton, D. Baggenstos, K. Kawamura, J. Severinghaus, Mean global ocean temperatures during the last glacial transition. *Nature* **553**, 39–44 (2018). doi:10.1038/nature25152 Medline

83. K. Lambeck, H. Rouby, A. Purcell, Y. Sun, M. Sambridge, Sea level and global ice volumes from the Last Glacial Maximum to the Holocene. *Proc. Natl. Acad. Sci. U.S.A.* **111**, 15296–15303 (2014). doi:10.1073/pnas.1411762111 Medline

84. A. Berger, M. F. Loutre, Insolation Values for the Climate of the Last 10 Million Years. *Quat. Sci. Rev.* **10**, 297–317 (1991). doi:10.1016/0277-3791(91)90033-Q

85. M. Crucifix, Palinsol: Insolation for palaeoclimate studies, R package version 0.93 (2016); https://bitbucket.org/mcrucifix/insol.

86. L. Bazin, A. Landais, B. Lemieux-Dudon, H. Toyé Mahamadou Kele, D. Veres, F. Parrenin, P. Martinerie, C. Ritz, E. Capron, V. Lipenkov, M.-F. Loutre, D. Raynaud, B. Vinther, A. Svensson, S. O. Rasmussen, M. Severi, T. Blunier, M. Leuenberger, H. Fischer, V. Masson-Delmotte, J. Chappellaz, E. Wolff, An optimized multi-proxy, multi-site

Antarctic ice and gas orbital chronology (AICC2012): 120–800 ka. *Clim. Past* **9**, 1715–1731 (2013). doi:10.5194/cp-9-1715-2013

87. D. Veres, L. Bazin, A. Landais, H. Toyé Mahamadou Kele, B. Lemieux-Dudon, F. Parrenin, P. Martinerie, E. Blayo, T. Blunier, E. Capron, J. Chappellaz, S. O. Rasmussen, M. Severi, A. Svensson, B. Vinther, E. W. Wolff, The Antarctic ice core chronology (AICC2012): An optimized multi-parameter and multi-site dating approach for the last 120 thousand years. *Clim. Past* **9**, 1733–1748 (2013). doi:10.5194/cp-9-1733-2013